Fluorescence imaging to assess the matrix metalloproteinase activity and its inhibitor *in vivo*

Zhihong Zhang*
Jie Yang*
Jinling Lu
Juqiang Lin
Shaoqun Zeng
Qingming Luo
Huazhong University of Science and Technology
Britton Chance Center for Biomedical Photonics
Wuhan National Laboratory for Optoelectronics
Wuhan 430074, China

Abstract. Matrix metalloproteinases (MMPs) are a kind of secretory proteinases. Degradation of the extracellular matrix (ECM) by MMPs enhances tumor invasion and metastasis. To monitor MMPs activity and assess the MMP inhibitor effects *in vivo*, we constructed a plasmid that encoded a secretory fluorescent sensor named DMC (DsRed2-MSS-CFP expressed from pDisplay vector) that DsRed2 and cyan fluorescent protein (CFP) linked by MMP substrate site (MSS). MDA-MB 435s cells highly expressing endogenetic secretory MMP were transfected with the DMC plasmid so that the DMC could be cleaved by endogenetic MMP and the fluorescence ratio of DsRed2 to CFP was decreased. Treating the cells with GM6001, an MMP inhibitor, blocked the cleavage of DMC and caused an increase of the DsRed2/CFP ratio. The same result was achieved by using an *in vivo* tumor model that stable DMC-expressing MDA-MB 435s cells inoculated onto the chorioallantoic membrane of developing chick embryos to form primary tumors on the membrane. Thus, the fluorescent sensor DMC is able to sensitively monitor MMP activity and assess MMP inhibitors for anticancer research *in vivo*. This proves a novel method to efficiently screen and assess the anticancer drug MMP inhibitor in living cells and *in vivo* tumor models. [DOI: 10.1117/1.2830659]

Keywords: matrix metalloproteinase (MMP); DsRed2; cyan fluorescent protein (CFP); optical imaging; MMP inhibitor.

Paper 07040SSR received Feb. 2, 2007; revised manuscript received Jul. 30, 2007; accepted for publication Aug. 1, 2007; published online Feb. 25, 2008. This paper is a revision of a paper presented at the SPIE Conference on Genetically Engineered and Optical Probes for Biomedical Applications IV, January 2007, San Jose, California. The paper presented there appears (unrefereed) in SPIE Proceedings Vol. 6449.

1 Introduction

Matrix metalloproteinases (MMPs) are a family of Zn^{2+}-dependent endopeptidases targeting extracellular matrix (ECM) compounds. The secreted MMPs anchor to the cellular surface to mediate ECM degradation and release of latent growth and angiogenic factors. Because of the ability of MMPs to degrade ECM proteins, the principal mechanism by MMPs' promoting tumor development has been thought to be the proteolytic breakdown of tissue barriers to invasion.[1] Moreover, MMP2- and MMP9-knockout mice[2] or tumor cells with downregulation of MMPs using RNAi[3,4] reduced tumor growth and invasion. MMP2 and MMP9 are particularly important, since they digest collagen, the main component of basement membranes.[5,6] Many MMP inhibitors have been designed to treat malignant tumors and other diseases associated with pathologic angiogenesis. Several inhibitors currently used in clinical development for cancer therapy include BB-2516, AG3340, COL-3, AE941, and so on.[7,8]

To study MMP activity for assessing MMP inhibitors *in vivo*, a near-infrared fluorescence probe has been designed and used to detect the activity of MMP 2.[9] This technique of measuring enzymatic activities has a profound impact on a variety of clinical and experimental studies, but the chemical synthesis of those probes is difficult and the cost is high. Compared with the chemical synthesized probes, a genetically encoded probe can easily be obtained by plasmid construction and used to set up a stable tumor model. In this paper, we design a genetically encoded fluorescent sensor named DMC (DsRed2-MSS-CFP expressed from pDisplay vector), that use DsRed2 and cyan fluorescent protein (CFP) linked by MMP substrate site (MSS) to indicate the MMP activity and evaluate the effect of MMP inhibitors *in vivo*.

MMPs are secreted as the proenzyme and activated outside of the cells. The sensor DMC was designed to detect the secreted MMPs. If the cells expressed high MMPs, the MMPs would act on the MSS site of DMC and result in DsRed2 and CFP separated and DsRed2 free from the cell's surface. Hence, the fluorescent signal of DsRed2 of tumor cells was weakened, and the fluorescent ratio of DsRed2 to CFP (DsRed2/CFP ratio) was very low. In reverse, if the cells expressed low MMPs or MMP activity was inhibited, the fluorescent sensor DMC would be intact. The fluorescent signals

*These authors contributed equally to this work.
Address all correspondence to Qingming Luo, Huazhong University of Science and Technology, Britton Chance Center for Biomedical Photonics, Wuhan National Laboratory for Optoelectronics, Wuhan 430074, China; Tel: +86 27 8779 2033; Fax: +86 27 8779 2034; E-mail: qluo@mail.hust.edu.cn

1083-3668/2008/13(1)/011006/6/$25.00 © 2008 SPIE

of both DsRed2 and CFP from DMC could be detected, and the DsRed2/CFP ratio was high. In this way, the DsRed2/CFP ratio could be used to reflect the level of MMP activity in DMC-expressing living cells.

In comparison with the fluorescence resonance energy transfer (FRET) sensor YFP-MSS-CFP^{display} published in our previous paper,[10] the choice of DsRed2 and CFP as the fluorescent pair to construct the genetically encoded fluorescent sensor DMC is due to the bright fluorescent signal of DsRed2 and less cross talk of the fluorescent signal between CFP and DsRed2. FRET imaging is easy for a cultured living cell using a confocal microscope. However, it is difficult to get a FRET signal using an *in vivo* optical imaging system because of the lower quality of an optical pathway system, such as a low numerical aperture objective and a light source with an LED or a lamp. This is hardly consistent the width imaging field range with high-resolution FRET images. Thus, the genetically encoded fluorescent sensor DMC combined with DsRed2/CFP ratio imaging is more suitable for monitoring the MMP activity *in vivo* than YFP-MSS-CFP^{display} combined with FRET imaging.

Furthermore, we used shell-less chick embryo chorioallantoic membrane (CAM) as a living subject for *in vivo* tumor imaging. CAM is a good model for *in vivo* optical imaging experiments because of its advantageous characteristics. CAM is an immunodeficiency animal model, so preparing various kinds of tumor models is easy. Compared with the tumor model prepared using nude mice, CAM is cheap and convenient to image, with a fast tumor growth rate. Therefore, it is very useful in the study of an *in vivo* antitumor drug screen. In this study, the fluorescent sensor DMC was used to detect MMP activity in living cells and in the shell-less CAM. This is a novel method for detecting extracellular MMP activity and screening the specific inhibitors of MMPs *in vivo*.

2 Materials and Methods

2.1 *Construction of Plasmids*

DsRed2 was amplified with the forward and reverse primers 5′-GGGA*AGATCT*ATGGCCTCCTCCGAGAACGTCATCACCG-3′ and 5′-CG*GGATCC*GCCTCCCTCCAGGAACAGGTGGTGGCGGC-3′. The amplified fragment was digested with *Bgl*II and *Bam*HI and cloned into pGEM-T. The forward and reverse primers of enhanced cyan fluorescent protein (ECFP) were 5′-CGGGATCCGTGCCCCTTAGCCTGTACAGCGGATCTAGAATGGTGAGCAAGGGCGAGGAGC-3′ and 5′-CAAGTCGACCATGCGGGCGGCGGTCACGAACTCCAGCAGG-3′, respectively. The polymerase chain reaction (PCR) products of ECFP were cloned into pGEM-T (Promega). The cloned cDNA of DsRed2 was selected with a right-inserted direction, and then the cloned cDNA of ECFP was conformed by sequencing. Next, the ECFP PCR product was digested with *Bam*HI and *Sal*I and subcloned at the *Bam*HI/*Sal*I site of pGEM-T-DsRed2. This subclone was digested with *Bgl*II and *Sal*I to produce the cDNA fragment of DsRed2-MSS-ECFP. This was subcloned into the pDisplay vector at the *Bgl*II and *Sal*I sites, and also into pET-28a at the *Bam*HI and *Xho*I sites.

2.2 *Expression and Purification of Recombinant Proteins*

The cDNA of DsRed2-MSS-ECFP was subcloned into vector pET-28a and then was transformed into BL21 (DE3) *E. coli* (Novagen Corp.) to produce the recombinant 6His-tagged DsRed2-MSS-CFP. Bacteria was cultured to $A_{600}=1$ and induced with 1 mM IPTG (isopropyl-beta-D-thiogalactopyranoside) for 16 h at 22°C. Then cells were disrupted by sonication in 30 ml lysis buffer (20 mM Tris. Cl, pH 7.9, 0.5 M NaCl, 1 mM PMSF) followed by centrifugation ($12{,}000\times$ g, 40 min). The recombinant protein was further purified by Ni-NTA resin (Qiagen). For further analysis, the recombinant protein was dialyzed in deionized water.

2.3 *Cell Culture and Transfection*

Samples of human breast tumor MDA-MB 435s cells were purchased from the Culture Center of Wuhan University (Wuhan, China), and human hepatic cancer HepG2 cells were kindly provided by the Immunology Laboratory of Tongji Medical College of Huazhong University of Science and Technology. The cells were routinely cultured in Dulbecco's modified eagle medium (DMEM) supplemented with 10% heat-inactivated fetal bovine serum (FBS). MDA-MB 435s and HepG2 cells were transfected with plasmid DMC by Sofast transfection reagent (Sunma Biotechnology Corp., Xiamen City, China), according to the instructions of the manufacturer. After transfection, DMC-expressing cells were screened by exposure to G418 (Sigma) 800 μg/ml for MDA-MB 435s cells and 400 μg/ml for HepG2 cells, and then stable DMC-expressing cells were cloned.

2.4 *Cellular Fluorescent Imaging*

The fluorescent images of DMC-expressing cells were created using an FV1000 Laser Confocal Scanning Microscope (Olympus, Japan) with a Plan Apo 60× oil immersion objective with a 1.42 numerical aperture. Each fluorescence channel was detected with a PMT (photo-multiplier tube), and Fluoview software was applied to this system. The CFP signals of the DMC-expressing cells were observed by using excitation light at 458 nm and emission at 465 to 485 nm. The DsRed2 signals of DMC-expressing cells were observed by using excitation light at 514 nm and emission at 580 to 650 nm.

2.5 *Fluorescence Spectroscopy*

The purification recombinant protein was incubated with 1 μM purified mature MMP2 (with a buffer of pH 7.5, 0.1 μM $ZnSO_4$, and 10 mM $CaCl_2$). The reaction mixtures were transferred to a 1-cm cuvette of a spectrofluorometer (LS-50B, Perkin-Elmer, Norwalk, Connecticut) at 37°C. Fluorescence emission spectra from 460 to 650 nm were recorded upon excitation at 433 nm (5-nm bandwidth).

2.6 *Western Blotting*

The purification DsRed2-MSS-CFP was incubated with or without 20 nM of the mature MMP2 for 30 min and then immediately incubated for 10 min at 95°C. The sample solutions were loaded for sodium dodecylsulfate-polyacrylamide gel electrophoresis. (SDS-PAGE) (10%). Pro-

teins were separated in the SDS-PAGE at 120 v for 2 to 3 h and subsequently transferred onto a polyvinylidene difluoride membrane (PVDF; Amersham) with a semidry blotting system. Following blotting, the membrane was probed with an anti-GFP (green fluorescent protien) antibody (1:2000; Clontech) in Tris-buffered saline with 0.5% Tween-20 (TBST). The immunoblot was then probed with horseradish peroxidase-conjugated secondary goat anti-rabbit IgG antibody (1:5000; Bio-Rad), and the bands were detected using the ECL Western blotting analysis system (Amersham).

2.7 *Chick Embryo Chorioallantoic Membrane (CAM) Model and Tumor Fluorescent Imaging*

Fertile chick eggs were incubated at saturation humidity for 72 h at 37.8°C. The embryos were then explanted into a shell-less culture using a method adapted from our previous report.[11] Briefly, a 10-cm-deep concave well was made using plastic food wrap fixed with elastic bands in the mouth of a polystyrene water cup ballasted with 30 ml of water. After 72 h incubation, the shells were then cracked against the edge of a glass vessel and the contents poured into the wells. Nearly always, the contents settled with the blastodisc uppermost and central. Then the cup was sealed with food wrap and placed in an incubator (37°C, 60% humidity). At day 10, 1×10^6 stable DMC-expressing MDA-MB 435s cells were explanted into CAM, and then GM6001 (Calbiochem Corp.), a kind of potent wide MMP inhibitor,[12] was add into 100 μl PBS solution. The solution was then added on the surface of the CAM near the tumor at a concentration of 0.4 μmol GM6001 per egg. As a negative control, the same number of cells was explanted into CAMs without GM6001. After three days of incubation, the fluorescence signals of the tumors were detected using a Leica MZ FL III fluorescence stereomicroscope with a mercury lamp (Leica, Germany). The DsRed2 (excitation filter 546/12 nm; barrier filter 560LP nm) and CFP (excitation filter 436/20 nm; barrier filter 480/40 nm) fluorescence-imaging pictures of the tumors were recorded with a color CCD (Evolution VF, Olympus Corp.)

3 Results and Discussion

3.1 *In Vitro Monitoring of MMP2 Cleavage of DsRed2-MSS-CFP Fusion Protein with Spectroscopic Measurements and Western Blot Analysis*

The cDNA of DsRed2-MSS-ECFP were constructed into pET-28a, which is able to express the recombinant DsRed2-MSS-CFP in *E. coli* BL21 (DE3) when induced with isopropyl-β-D-thiogalacto-pyranoside (IPTG) [Fig. 1(a)]. Then the recombinant protein was purified through an Ni-NTA column after being induced with 1 mM IPTG. The peptide of VPLSLYSG in MSS was chosen because of its high k_{cat}/K_m value for MMP2.[13] To determine the cleavage sensitivity of the fusion protein DsRed2-MSS-CFP to MMP2, we first examined it *in vitro*. As show in [Fig. 1(b)], fluorescence resonance energy transfer (FRET) from CFP to DsRed2 took place[14] when the DsRed2-MSS-CFP was intact. If MMP2 cleaved the linker peptide between CFP and DsRed2, FRET would be abolished. The changes of FRET in response to MMP2 cleavage were measured with a spectrofluorometer at

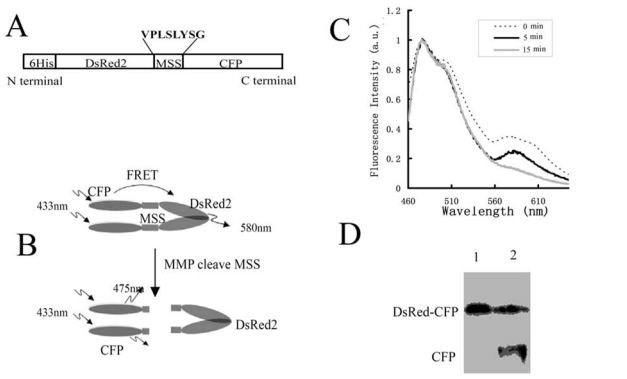

Fig. 1 Schematic drawing and analysis of fusion protein DsRed2-MSS-CFP *in vitro*. (a) Schematic representation of the 6His-tagged DsRed2-MSS-CFP. The cDNA of DsRed2-MSS-CFP were constructed into pET-28a, which is able to express the recombinant 6His-tagged DsRed2-MSS-CFP in *E.coli* BL21 (DE3) when induced with IPTG. (b) Conceptual drawing of a fluorescent biosensor DsRed2-MSS-CFP for detecting MMP activity. When the DsRed2-MSS-CFP is intact, the donor CFP absorbs energy from the excitation source (433 nm) and then nonradiatively transfers the energy to the acceptor DsRed2, which in turn emits a fluorescent photon (580 nm). When DsRed2-MSS-CFP is cleaved by MMPs, the fluorescence intensity of the donor's emission wavelength will increase at 475 nm, and little fluorescence of the acceptors' emission wavelength can be deteced at 580 nm. (c) The purification DsRed2-MSS-CFP was incubated with 20 nM of the mature MMP2 in a buffer of pH 7.5, 0.1 μM $ZnSO_4$, and 10 mM $CaCl_2$. The reaction mixtures were transferred to a 1-cm cuvette of a spectrofluorometer (LS-50B, Perkin-Elmer, Norwalk, Connecticut) at 37°C. Fluorescence emission spectra from 460 to 650 nm excited at 433 nm (5-nm bandwidth) were recorded before and after reacting 5 and 15 minutes later, respectively. The spectra were normalized at 475 nm. (d) A Western blot was used to confirm that DsRed2-MSS-CFP was cleaved by MMP2. Lane 1 is a Western blot of the DsRed2-MSS-CFP in the absence of MMP2. Lane 2 is the product of DsRed2-MSS-CFP in the presence of MMP2.

37°C. Figure 1(c) shows the emission spectra of the purified DsRed2-MSS-CFP fusion protein with an excitation wavelength of 433 nm. The two emission peaks of DsRed2-MSS-CFP occurred at 476 nm and 580 nm, corresponding to peaks of CFP and DsRed2, respectively. This result indicated that FRET from CFP to DsRed2 occurred and that the DsRed2-MSS-CFP fusion protein was intact. After adding 20 nM MMP2 into the solution of DsRed2-MSS-CFP, the emission peak of DsRed2-MSS-CFP at the wavelength of 580 nm disappeared 15 min later. Furthermore, Western blotting analysis [Fig. 1(d)] demonstrated that DsRed2-MSS-CFP was cleaved by MMP2. *In vitro* analysis indicated that DsRed2-MSS-CFP could be used as a fluorescence sensor to detect MMP2 activity. For *in vitro* monitoring of MMP2 cleavage of the DsRed2-MSS-CFP fusion protein with spectroscopic measurements, we have to use the FRET property of DsRed2-MSS-CFP. Otherwise, the DsRed2/CFP ratio of the integrated or cleaved DsRed2-MSS-CFP fusion protein will be the same in the solution.

3.2 *Localization of Fluorescence Sensor*

MMPs are secreted as proenzymes and can degrade extracellular matrix (ECM) components once activated. To test the level of MMPs in the living cells, we chose a vector pDisplay

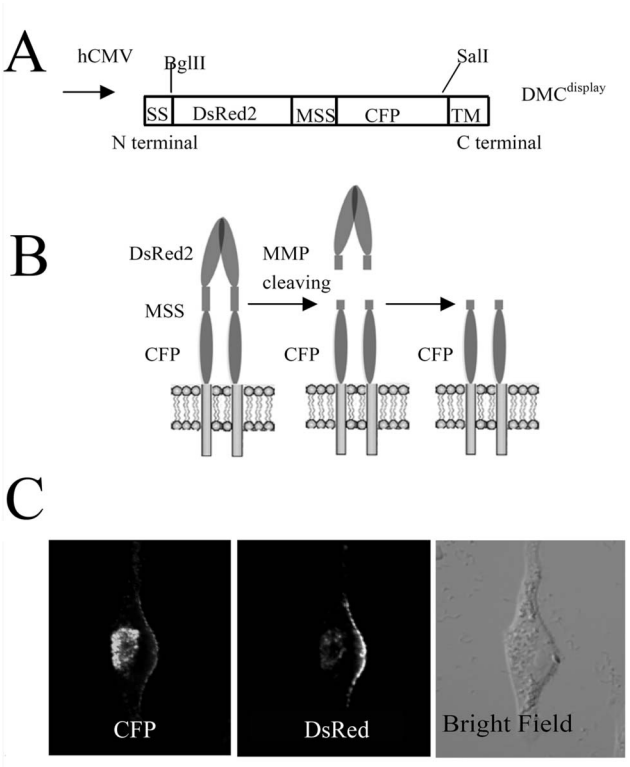

Fig. 2 Schematic drawing and localization of fluorescence sensor DMC in living cells. (a) DMC consists of a secretion signal (SS) at the N-terminus and PDGF transmembrane (TM) domain at the C terminal. (b) Schematic representation of a part of DMC molecular localization on the cellular surface. Because the active MMP2 can cleave MSS in the DMC, the DsRed2 signal will disappear if the cell itself has highly expressed MMP2. (c) Confocal fluorescent images of DMC-expressing HepG2 cells. The CFP signal of DMC-expressing cells was observed by excitation light at 458 nm and emission at 465 to 485 nm. The DsRed2 signal of DMC-expressing cells was observed by excitation light at 514 nm and emission at 580 to 650 nm.

(Invitrogen Corp.) that is a mammalian expression vector, allowing the protein under investigation to enter the secretory pathway and anchor on the cellular surface [Fig. 2(a)]. Proteins expressed from pDisplay are fused at the N-terminus to the murine Ig κ-chain signal sequence, which directs the protein to the secretory pathway, and at the C-terminus to the transmembrane domain of platelet derived growth factor receptor (PDGFR), which anchors the protein to the plasma membrane, displaying it on the extracellular side. The expressing probes anchor on the cellular surface, where fluorescence probes can be cleaved by secreted MMP [Fig. 2(b)]. After the DMC was cleavaged by MMPs, DsRed2 was cut off and free from the DMC-expressing cells, while CFP still remained in the cells. Thus, the MMP activity of tumor cells could be traced through monitoring the decrease of the fluorescent signal of DsRed2. To provide further support on the subcellular distribution of expressed fluorescence proteins, the vector of pDisplay-DMC was transfected into HepG2 cells with low expressing MMPs. As shown in Fig. 2(c), fluorescent signals in the cellular secretory pathway and on the cellular surface were visualized in an optical section obtained by the confocal microscope.

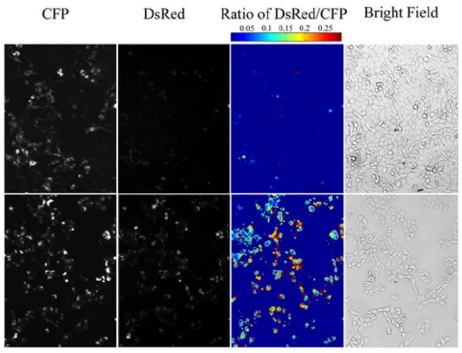

Fig. 3 The fluorescence ratio images of DsRed2 to CFP reflected the effect of GM6001 inhibition on MMP activity in living cells. After 72 h treatment with 40 μM GM6001, cells were observed at the CFP channel and DsRed2 channel, and the images of control cells (without GM6001 treatment) also were recorded. The top row of images is the control group, and the bottom row of images is the GM6001-treated group. The fluorescence ratio images of DsRed2 to CFP were calculated with MATLAB 7.0, and pseudocolor represented the relative ratio value.

In Fig. 2(c), the confocal fluorescent images of DMC-expressing HepG2 cells showed the most fluorescence signal of CFP and DsRed2 co-localized at the plasma membrane and the secretory pathway in the same single cells. Because HepG2 cells only low-express MMPs and were not a completely negative control, some regions in the plasma membrane at the tail end of the cell appear with only a CFP signal and no DsRed2 signal. Furthermore, DsRed2 required many hours to attain full fluorescence. CFP forms a chromophore rapidly after translation (half time=49 min).[15] DsRed2 takes longer to develop a coloration (half time=6.5 h).[16] If DsRed2 was used to tag the secretory protein, the fusion protein should be secreted prior to maturation for fluorescence.[17] Thus, slow maturing of DsRed2 in living cells resulted in the different fluorescent intensity of CFP and DsRed2 inside the cell and at the cell surface in the same single cell, despite the fact that DMC-expressing HepG2 cells should contain equal parts of CFP and DsRed2.

3.3 *Using the DsRed2/CFP Ratio to Detect MMP Inhibitor Effects in Living Cells*

The fluorescence sensor DMC was designed to trace MMP activity in living cells and small animals. When the cells excrete MMP2, the sensor DMC expressed on the surface of the cell plasma member or on the secretory pathway will be cleaved by the MMP2. Thus, DsRed2 is freed from the cells so that it is barely detected by fluorescent imaging. MDA-MB 435s cells are chosen because they highly express MMP2 and also produce MMP1, MMP3, MMP9, MMP14, MMP15, and MMP16.[18] Figure 3 shows that the fluorescence signals of DMC-expressing MDA-MB 435s cells were simultaneously detected in the CFP and DsRed2 channels. MMP inhibitor GM6001 could dramatically increase the DsRed2 signal after 72 h of treatment. This indicated that GM6001 could efficiently inhibit the MMPs activity so that the new procreant DMC could be kept intact in living MDA-MB 435s cells.

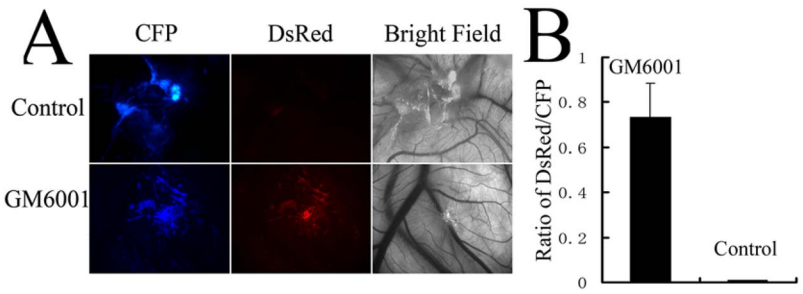

Fig. 4 *In vivo* optical images for assessing the effect of MMP inhibitors. (a) MDA-MB 435s cells that expressed DMC were explanted on the shell-less chick embryo chorioallantoic membrane (CAM). The tumor was treated by MMP inhibitor GM6001 0.4 μmol for 3 days, and GM6001 is absent in the control group. The MMP activity during tumor growth was reflected through monitoring the fluorescent signals of CFP and DsRed2 simultaneously. (b) The DsRed2/CFP ratio in CAMs were calculated after 0.4 μmol GM6001 treatment of the tumor for 3 days. Data represent three repetitions.

3.4 *Detecting MMP Inhibitor Effects in CAMs with DsRed2 and CFP Imaging*

In vivo imaging of MMPs will be very useful for medical target assessment. In this experiment, we used the chick embryo CAM in a shell-less culture as our experimental model. This model has an advantage of allowing direct observation of fluorescence in the embryo surface without interference by the skin or other tissue. Monitoring the fluorescence signals of CFP and DsRed2 simultaneously reflected the MMP inhibitor effect during tumor growth on CAM. The fluorescent images of CAM were obtained after 3 days of treatment with or without GM6001 (Fig. 4). The tumor treated with GM6001 [the bottom row of Fig. 4(a)] yielded a brighter DsRed2 fluorescence signal than the control tumor [the top row of Fig. 4(a)]; however, the CFP signals of the two groups had no obvious difference. Thus, we still use the DsRed2/CFP ratio to more exactly reflect the effect of the MMP inhibitor [Fig. 4(b)], and the results were taken from experiments three times repeated. MMP inhibitor GM601 could obviously increase the DsRed2/CFP ratio because it inhibited the cleavage of the sensor by active MMPs.

In this paper, we detected the MMP activity *in vivo* using a fluorescence stereomicroscope, a kind of optical imaging system with a larger imaging field and lower resolution than the confocal microscope. Although DMC is a FRET probe, it is difficult to detect a FRET signal *in vivo* by fluorescence stereomicroscope because of the low numerical aperture objective and because the light source is a mercury lamp. Furthermore, the FRET efficiency of DsRed2/CFP is much lower than YFP/CFP.[10] Thus, we used the DsRed2/CFP ratio to reflect the MMP activity and did not detect the FRET efficiency of DMC.

Here, the CFP signal could be used as an internal reference to eliminate the error due to the difference of fluorescent sensor expression in various cells or the difference of imaging focus, and this could tell us where the tumor cells are if the cells highly secreted MMPs. This supposes that if we construct an expressing display vector containing only DsRed2-MSS, it also can be cleaved by MMPs. However, if DsRed2-MSS was transfected into the tumor cells with high secretory MMPs, we cannot detect an obviously fluorescent signal and we do not know whether this is due to the low transfection efficiency or high MMP activity. According to the mechanism of FRET, the fluorescence signal of CFP will increase if DMC was cleaved by MMPs. Because of this, the DsRed2/CFP ratio could generate a high contrast between its intact and cleaved components. If the cells low expressed MMPs, or if MMP activity was inhibited by an MMP inhibitor, DMC would stay intact and the cells could be detected with the fluorescence signals of both DsRed2 and CFP. The DsRed2/CFP ratio would be high. If the cells highly secrete MMPs, DMC would be cleaved, and the cells would appear with obviously decreased fluorescent signal of DsRed2 and lightly increased fluorescent signal of CFP, so the DsRed2/CFP ratio would decrease. We cannot directly compare the fluorescent signal of DsRed2 or CFP alone because the different expressing of the cells and the imaging focus will effect the fluorescent intensity of DsRed2 and CFP. Thus, the DsRed2/CFP ratio is a good approach to reflect the activity of MMPs *in vivo*.

4 Conclusion

In this study, we have demonstrated that the fluorescence sensor DMC can be used to monitor MMP cleavage activity and to analyze MMP inhibitor effects in living cells and in CAMs. Highly sensitive and specific fluorogenic substrates were designed as sensors with the ability to detect small-molecule inhibitors. Fluorescence imaging of DMC in the CAM was sensitive to the MMP inhibitor. This method could be very valuable for developing effective medicines for cancer therapy and also for evaluating inhibitors *in vivo*. Compared with the YFP-MSS-CFP^{display}, a genetically encoded surface-displayed FRET sensor to detect MMP activity in living cells,[10] DMC is more suitable for *in vivo* imaging by the fluorescence stereomicroscope because of the infrequent cross talk between the fluorescent signals of DsRed2 and CFP. Despite the lower FRET efficiency of the DsRed2/CFP pair than the YFP/CFP pair, the DsRed2/CFP ratio of DMC-expressing cells still could sensitively reflect the MMP activity in living cells and in the *in vivo* tumor model.

In the living cells and CAM tumor models, the CFP and DsRed2 signals were simultaneously detected to assess the effect of the MMP inhibitor. According to the CFP signal, we can continuously detect the position and size of tumors even if the DsRed2 signal disappeared due to the cleavage of DMC by the active MMPs. On the other hand, CFP could be used as

an internal reference to eliminate the error due to the difference of DMC expression. This genetically encoded probe has a good application perspective for assessing the MMP inhibitor effect *in vivo* and *in vitro*. Many MMP inhibitors have undergone clinical trials, such as BB-2516, AG3340, COL-3, and AE941.[19] The currently available approaches to monitor MMP inhibition therapies are based on indirect evidence of therapy, such as tumor size, histological changes, and possibly MMP levels in blood or tumor tissue measured, and these take a long time. These approaches do not provide a reliable result for assessing inhibition of MMP activity *in vivo*. This study provides a direct method of molecular target assessment, and it will benefit MMP inhibitor studies that are under way.

Acknowledgments

This work was supported by the National Natural Science Foundation of China (Grant Nos. 90508003 and 60440420131), the National Key Technologies Research and Development Program of China (Grant No. 2005BA711A04), Program for Changjiang Scholars and Innovative Research Team in University, and the Scientific Research Foundation for the Returned Overseas Chinese Scholars, State Education Ministry (Z. Zhang).

References

1. I. Stamenkovic, "Matrix metalloproteinases in tumor invasion and metastasis," *Semin Cancer Biol.* **10**, 415–433 (2000).
2. G. M. Longo, W. Xiong, T. C. Greiner, Y. Zhao, N. Fiotti, and B. T. Baxter, "Matrix metalloproteinases 2 and 9 work in concert to produce aortic aneurysms," *J. Clin. Invest.* **110**, 625–632 (2002).
3. J. Yuan, C. M. Dutton, and S. P. Scully, "RNAi mediated MMP-1 silencing inhibits human chondrosarcoma invasion," *J. Orthop. Res.* **23**, 1467–1474 (2005).
4. S. S. Lakka, C. S. Gondi, N. Yanamandra, W. C. Olivero, D. H. Dinh, M. Gujrati, and J. S. Rao, "Inhibition of cathepsin B and MMP-9 gene expression in glioblastoma cell line via RNA interference reduces tumor cell invasion, tumor growth, and angiogenesis," *Oncogene* **23**, 4681–4689 (2004).
5. M. A. Moses, "The regulation of neovascularization of matrix metalloproteinases and their inhibitors," *Stem Cells* **15**, 180–189 (1997).
6. M. Nguyen, J. Arkell, and C. J. Jackson, "Human endothelial gelatinases and angiogenesis," *Int. J. Biochem. Cell Biol.* **33**, 960–970 (2001).
7. M. Egeblad and Z. Werb, "New functions for the matrix metalloproteinases in cancer progression," *Nat. Rev. Cancer* **2**, 161–174 (2002).
8. C. Bremer, C. H. Tung, and R. Weissleder, "*In vivo* molecular target assessment of matrix metalloproteinase inhibition," *Nat. Med.* **7**, 743–748 (2001).
9. C. Bremer, S. Bredow, U. Mahmood, R. Weissleder, and C. H. Yung, "Optical imaging of matrix metalloproteinase–2 activity in tumors: feasibility study in a mouse model," *Radiology* **221**, 523–529 (2001).
10. J. Yang, Z. H. Zhang, J. Q. Lin, J. L. Lu, B. F. Liu, S. Q. Zeng, and Q. M. Luo, "Detection of MMP activity in living cells by a genetically encoded surface-displayed FRET sensor," *Cell Res.* **1773**, 400–407 (2007).
11. S. B. Zhuo, Z. H. Zhang, Q. Liu, S. Q. Zeng, and Q. M. Luo, "The application of optical imaging: Studying the photodynamic effect of tumor *in vivo*," *Prog. Biochem. Biophys.* **32**, 969–974 (2005).
12. B. Winding et al., "Synthetic matrix metalloproteinase inhibitors inhibit growth of established breast cancer osteolytic lesions and prolong survival in mice," *Clin. Cancer Res.* **8**, 1932–1939 (2002).
13. B. E. Turk, L. L. Huang, E. T. Piro, and L. C. Cantley, "Determination of protease cleavage site motifs using mixture-based oriented peptide libraries," *Nat. Biotechnol.* **19**, 661–667 (2001).
14. M. G. Erickson, D. L. Moon, and D. T. Yue, "DsRed as a potential FRET partner with CFP and GFP," *Biophys. J.* **85**, 599–611 (2003).
15. A. Gordon, A. Colman-Lerner, T. E. Chin, K. R. Benjamin, R. C. Yu, and R. Brent, "Single-cell quantification of molecules and rates using open-source microscope-based cytometry," *Nat. Methods* **4**, 175–181 (2007).
16. B. J. Bevis and B. S. Glick, "Rapidly maturing variants of the discosoma red fluorescent protein (DsRed)," *Nat. Biotechnol.* **20**, 83–87 (2002).
17. M. Maruyama, T. Nishio, T. Yoshida, C. Ishida, K. Ishida, Y. Watanabe, M. Nishikawa, and Y. Takakura, "Simultaneous detection of DsRed2-tagged and EGFP-tagged human β-interferons in the same single cells," *J. Cell. Biochem.* **93**, 497–502 (2004).
18. T. A. Giambernardi, G. M. Grant, G. P. Taylor, R. J. Hay, V. M. Maher, J. J. McCormick, and R. J. Klebe, "Overview of matrix metalloproteinase expression in cultured human cells," *Matrix Biol.* **16**, 483–496 (1998).
19. C. M. Overall and O. Kleifeld, "Validating matrix metalloproteinases as drug targets and anti-targets for cancer therapy," *Nat. Rev. Cancer* **6**, 227–239 (2006).